Biochimica et Biophysica Acta, 1015 (1990) 53–60
Elsevier

BBABIO 43100

EPR observation of carbon monoxide dehydrogenase, methylreductase and corrinoid in intact *Methanosarcina barkeri* during methanogenesis from acetate

Joseph A. Krzycki and Roger C. Prince

Exxon Research and Engineering Company, Annandale, NJ (U.S.A.)

(Received 17 July 1989)

Key words: Methanogenesis; ESR; Carbon monoxide dehydrogenase; Methylreductase; Corrinoid

Carbon monoxide dehydrogenase, corrinoid, and methylreductase can be observed with EPR spectroscopy during active methanogenesis from acetate in whole cells of *Methanosarcina barkeri*. During methanogenesis, center 2 of carbon monoxide dehydrogenase ($g = 2.01$, 1.91, 1.76) shows similar changes to those seen in the isolated enzyme upon addition of CO, with the appearance of a new feature at $g = 1.73$. This indicates that the cleavage of acetate yields a moiety that carbon monoxide dehydrogenase recognizes as CO. Cyanide rendered center 2 of carbon monoxide dehydrogenase EPR-silent, suggesting that this potent inhibitor of methanogenesis from acetate acts at the level of this enzyme. Cyanide also induced formation of two very fast relaxing centers with overlapping rhombic signals in the iron-sulfur region of the spectrum. Transient electron flow through iron-sulfur clusters could be correlated with methanogenesis, and could be prevented by iodopropane or cyanide. Cells before and after methanogenesis possessed a putative nickel signal at $g = 2.28$, 2.27 and 2.18. During methane production this signal was replaced by an axial signal ($g = 2.24$, 2.05). These signals are similar to those reported for methylreductase from *Methanobacterium*. EPR-detectable corrinoid underwent no significant change during methanogenesis and was unaffected by the presence of either cyanide or iodopropane.

Introduction

The few substrates which have been demonstrated to serve as precursors of biologically produced methane are generally one-carbon compounds such as carbon dioxide, methanol or methylamine. Only one compound possessing a carbon–carbon bond can act as a direct precursor of methane, and this is acetic acid [1]. During methanogenesis from acetate, methane is produced primarily from the methyl group, while carbon dioxide is derived from the carboxyl [2]. A schematic describing how this is accomplished and coupled to ATP formation is presented in Fig. 1. The splitting of the acetate carbon–carbon bond apparently occurs following an ATP-dependent activation of acetate [3], probably to acetyl-CoA [4,5] and leads to generation of methyl-coenzyme M and a carbonyl moiety [3,6–8]. Current models of energy conservation during this catabolic reaction invoke chemiosmosis, the membrane potential being generated by a membrane-bound electron transport chain connecting oxidation of the carbonyl moiety to the reduction of methyl-CoM (Refs. 7, 9, 10, Fig. 1).

Numerous studies support that carbon monoxide dehydrogenase catalyzes the oxidation of the carbonyl moiety, as well as mediating the actual splitting of the acetyl carbon–carbon bond [1]. Carbon monoxide dehydrogenase activity is highest in cells cultured on acetate relative to other substrates [11]. Precipitation of the enzyme by antibodies in cell free extract removes both CO dehydrogenase activity and acetate-dependent methanogenesis [3]. Cyanide, a potent inhibitor of methane formation from acetate, but not other substrates [12], will also inhibit CO oxidation by CO dehydrogenase at similar concentrations [13]. Carbon monoxide dehydrogenase has been isolated from organisms in which it is apparently involved in the synthesis [14,15] or the breakdown [13,16,17] of acetyl-CoA; in all cases it is a nickel/iron-sulfur enzyme. In *Clostridium thermoaceticum*, one of the former type, the isolated enzyme can catalyze the exchange of CO_2 into acetyl-CoA [18].

Correspondence (present address): J.A. Krzycki, Department of Microbiology, Ohio State University, Columbus, OH 43210, U.S.A.

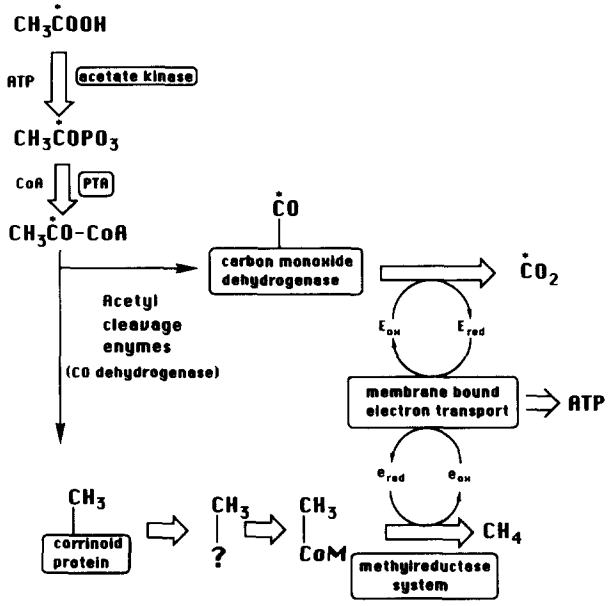

Fig. 1. Carbon and electron flow coupled to ATP formation during methanogenesis from acetate. The number of methylated intermediates between the corrinoid protein and methylcoenzyme M are unknown. Carbon monoxide dehydrogenase is implicated in both the cleavage of acetyl-CoA and oxidation of the subsequent carbonyl group.

A corrinoid protein is thought to directly receive methyl groups following the cleavage of acetate prior to the methylation of coenzyme M. Corrinoid levels are quite high in methanogens, especially in *Methanosarcina* [19]. Iodopropane is an especially potent inhibitor of methanogenesis from acetate [20,21]. Inhibition is easily reversed by exposure to light, consistent with inhibition occurring via propylation of corrinoid cobalt. Radioactive acetate has recently been shown to label part of the corrinoid pool in methanogenic extracts of *Methanosarcina* [23].

Tracer experiments have shown that methyl-CoM is the final intermediate of methanogenesis from acetate [3,6]. The reduction of methyl-CoM to methane is catalyzed by methylreductase, an enzyme which possesses a unique nickel tetrapyrrole, Factor F_{430} [23]. The direct reductant of methyl-CoM is HTP, mercaptoheptanoylthreonine phosphate. Methane and the mixed disulfide of HTP and coenzyme M are released as the products of methylreductase [24,25].

We have found that several of the components implicated in the formation of methane from acetate, such as carbon monoxide dehydrogenase, methylreductase and corrinoid, are paramagnetic and can be observed in intact cells and extracts of *Methanosarcina barkeri* using electron paramagnetic resonance spectroscopy. We therefore studied these paramagnetic centers during methanogenesis from acetate, and during inhibition by cyanide and iodopropane.

Materials and Methods

Growth of organism and preparation of cell suspensions or extracts

Methanosarcina barkeri strain MS (DSM 800) was cultivated in 40 liters of phosphate-buffered medium with acetate as sole carbon and energy source, as previously described [26]. After 12–14 days of growth the active cells were allowed to settle and the majority of the cleared medium displaced with positive nitrogen pressure. The remaining 0.5 liter of cells was cooled on ice and centrifuged anaerobically at $5000 \times g$ under a 95 : 5 nitrogen/hydrogen gas phase. The cells were then resuspended in anaerobic 50 mM potassium phosphate buffer (pH 7.0) with 150 mM NaCl and again centrifuged. The pellet was suspended in 50 ml of the same buffer, flush/evacuated with nitrogen and kept on ice until the experiments were performed.

Cell extract was prepared from cells harvested in the same manner, but washed with 50 mM Mops buffer (pH 7.0) prior to passage of a 1 g cells/2 ml buffer suspension through a French pressure cell at 20000 p.s.i. The lysate was collected anaerobically under hydrogen, then centrifuged at $27000 \times g$ to obtain the supernatant. Carbon monoxide dehydrogenase was isolated as described previously [26]. Protein was determined by Coomassie blue binding [27]. Cobalt was determined by plasma emission spectroscopy by the Analytical division of Exxon Corporate Research Laboratories. Methane was determined using a Varian 6500 gas chromatograph equipped with a Poropak R column and a flame ionization detector.

Electron paramagnetic resonance spectra

Spectra were recorded using a Varian E-109 Spectrometer (Varian Instruments, Palo Alto, CA) equipped with an EIP model 548A microwave frequency counter (EIP Industries, San Jose, CA). Samples were cooled using liquid helium delivered to an ESR-900 cryostat (Oxford Instruments, Bedford, MA). Unless otherwise indicated, the following parameters were used during recording of spectra: 1 mT modulation amplitude, 80 mT/min scan rate, 0.128 s time constant, 100 kHz modulation frequency, and microwave frequency of 9.25 GHz. Cell suspension experiments were conducted in 70 ml vials under a nitrogen atmosphere. Additions of acetate, iodopropane or cyanide were made prior to the addition of 5 ml of chilled cell suspension. Reactions were initiated by transfer of the vials from ice to a 37 °C water bath. Methane was monitored by removal of 25 µl of gas phase, and at indicated timepoints 0.3 ml of cell suspension were removed and transferred to a nitrogen gassed EPR tube. The tube was then immediately frozen in chilled isooctane (−50 °C), then transferred to liquid nitrogen. In order to prevent possible cleavage of photolabile bonds, reactions were per-

formed in dim light and the EPR tubes were kept in covered Dewar flasks. During experiments with iodopropane, vials were kept covered with aluminum foil prior to light reversal of inhibition.

Results

Identification of some EPR-detectable centers in cell-free extracts

EPR spectra taken at 12 K of *M. barkeri* extracts, prepared under hydrogen, display several prominent signals (Fig. 2A and B). One feature, at $g = 2.25$, was of lineshape and position appropriate for the $g_\perp$ of a Co(II) corrinoid, as illustrated by comparison to spectra of Co(II) cobalamin (Fig. 2C and D). Similar spectra have been obtained of Co(II) corrinoid proteins isolated from methanogenic bacteria [28–30], although an unusually low $g_\perp$ value was reported by Lino et al. [28]. The broad $g = 2.25$ line observed in extracts and Co(II) cobalamin at 0.1 mW (Fig. 2, traces A and C) sharpened substantially upon application of higher microwave power (Fig. 2, traces B and D). Spectra recorded at 70 K of cell extracts under hydrogen were dominated by the lineshape of Co(II) corrinoid.

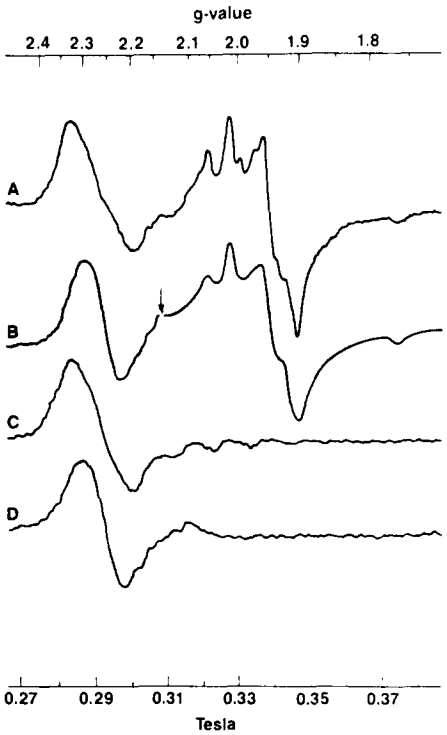

Fig. 2. EPR spectra of *M. barkeri* extract and Co(II) cobalamin recorded at 12 K. (A) 28 mg protein/ml cell free extract in 50 mM Mops buffer (pH 7.0), incubated under hydrogen. 0.1 mW microwave power, gain set at $2 \cdot 10^4$. All other instrument settings are as described in Materials and Methods. (*B*) As in (A), but 100 mW power. Gain was shifted from $8 \cdot 10^3$ to $1.25 \cdot 10^3$ at the arrow. (C) Co(II) corrinoid in 50 mM Tris (pH 8.0) obtained by partial reduction of 0.5 mM hydroxycobalamin by dithiothreitol. 0.1 mW microwave power, gain of $1.6 \cdot 10^4$. (D) Same as (C), but 100 mW power, gain of $10 \cdot 10^3$.

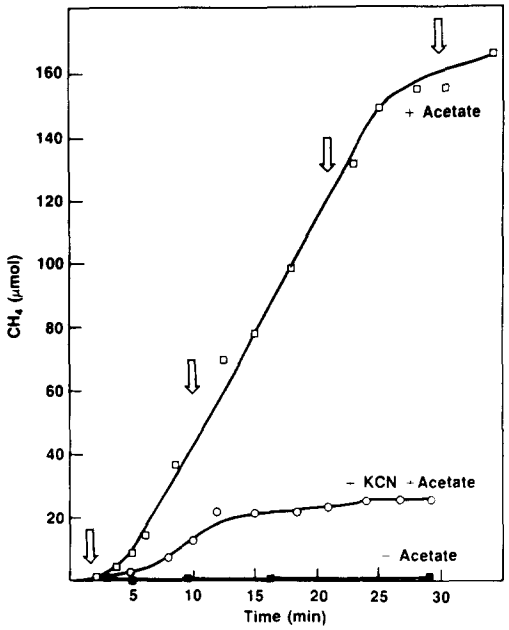

Fig. 3. Methane formation by a cell suspension of *M. barkeri*. 5 ml of a cell suspension on ice was transferred to a nitrogen-flushed 70 ml vial and incubated at 37 °C. If added, 40 mM acetate and/or 50 μM KCN were present. At the arrows, samples were removed and frozen for spectral analysis.

Complex signals are seen in spectra of extracts taken at temperatures up to 40 K (Fig. 2). These arise primarily from iron-sulfur proteins such as hydrogenase [31], carbon monoxide dehydrogenase [26], and the several iron-sulfur clusters which have been identified in the membrane fraction of *M. barkeri* [32]. The power and temperature saturation characteristics of the $g = 1.76$ line, and its behavior during redox titrations of extracts, allow its identification as the g_x feature of the rhombic signal ($g = 2.01$, 1.91, 1.76) from center 2 of carbon monoxide dehydrogenase [26].

EPR-detectable changes in intact cells during methanogenesis from acetate

The Co(II) corrinoid and carbon monoxide dehydrogenase signals, both arising from participants in methane formation from acetate, could also be readily identified in suspensions of intact, log-phase, cells prepared under anaerobic conditions. In order to observe these centers during active methanogenesis, cell suspensions on ice were transferred to nitrogen flushed vials at 37 °C and given a pulse of sodium acetate. After a lag of 4 min, the rate of methane formation was linear for approx. 20 min (Fig. 3); little methane was observed in samples incubated without acetate. Samples for EPR were removed at the indicated times and the resultant spectra are displayed in Fig. 4. All spectra were dominated by the $g_\perp$ of Co(II) corrinoid and center 2 of carbon monoxide dehydrogenase, but control samples (without acetate) showed no changes during incubation.

Changes in the EPR spectra of cells, after the addition of acetate, but before the onset of active methane formation, became more pronounced during linear methane formation. 1 min after the addition of acetate (Fig. 4) a shoulder is detectable at higher field near the $g = 1.76$ feature of center 2. This feature intensified during steady state methane formation, as seen at 10 and 21 min after the addition of acetate. The appearance of this feature correlates with a decrease in the intensity of the $g = 1.76$ line by approximately 50%. 30 min after addition of acetate, after methane formation had nearly ceased, the $g = 1.76$ line had returned to its original intensity, while the $g = 1.73$ feature was no longer discernible. Brief exposure of purified carbon monoxide dehydrogenase to carbon monoxide results in a similar loss of the $g = 1.76$ line and appearance of the line at $g = 1.73$ [26].

Several other changes were notable in EPR-detectable centers. Before the onset of methane formation there is evidence of a new peak near $g = 1.95$. During linear methane formation the signal intensity at $g = 1.95$ has greatly increased. Since this is a typical value for the g_y of iron-sulfur clusters, it suggests electron flow through such clusters during active methanogenesis. Again, this effect was transient, and following cessation of methanogenesis the cells returned to essentially their resting state.

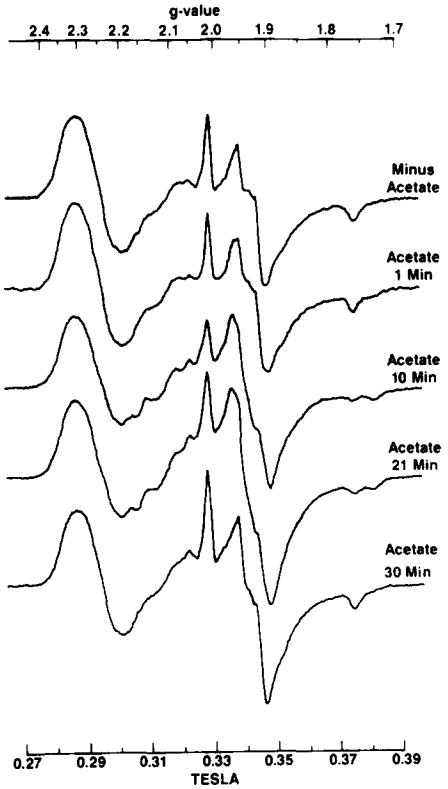

Fig. 4. EPR spectra recorded at 12 K of cells before, during, and after methanogenesis. Samples were removed from the suspension in Fig. 3 at the times indicated. The minus acetate sample was taken from a suspension incubated for 30 min without substrate. All other spectra were taken from the vial pulsed with acetate. Microwave power was 10 mW, gain of all spectra was $8 \cdot 10^4$.

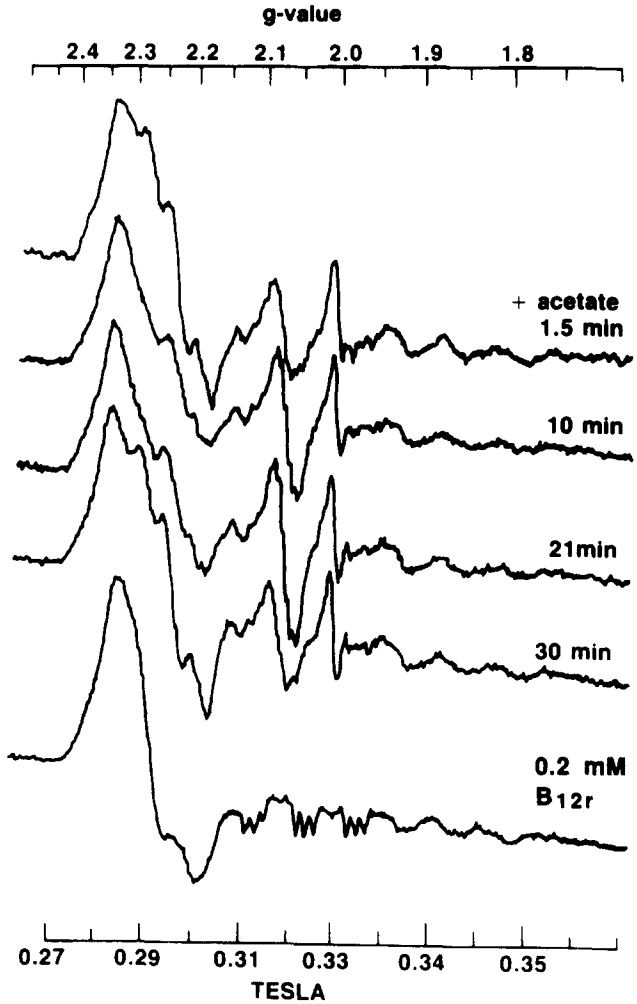

Fig. 5. EPR spectra recorded at 70 K of cells during and after methanogenesis from acetate. The samples are those from the cell suspension in fig. 3 and were removed at the times indicated. Spectra of cells without acetate were identical to the top spectrum. The spectrum of Co(II) cobalamin (B-12r) was obtained by quantitative reduction of hydroxocobalamin with dithiothreitol. Power in all cases was 10 mW, gain for cell samples was $2 \cdot 10^4$ and $1.6 \cdot 10^4$ for Co(II) cobalamin.

Surprisingly, we could detect little change in the intensity of $g_\perp$ of Co(II) corrinoid during methanogenesis. At most, we could detect a decrease of 8% measured from baseline to top of the $g = 2.33$ peak, which was within sampling error. Spectra recorded at 70 K (Fig. 5) of the same samples examined in Fig. 4 lead to the conclusion that the pool of EPR-detectable corrinoid remains relatively constant both before, during and after methanogenesis from acetate. Comparison of the peak intensity of the Co(II) corrinoid signal in intact cells to that of Co(II) cobalamin under identical, nonsaturating conditions yielded a concentration of 0.12 mM Co(II) corrinoid in the cell suspension. Cobalt in

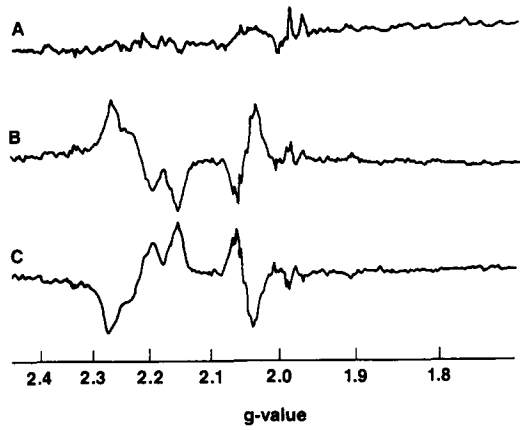

Fig. 6. Difference spectra of cells before, during, and after methanogenesis from acetate. The spectra used for data manipulation were those in Fig. 5, all recorded at 70 K. (A) Cells incubated for 4 min at 37 °C without acetate minus cells incubated for 1 min in the presence of acetate, before the onset of active methanogenesis. (B) Cells after cessation of linear methane formation (30 min, with acetate) minus cells during active methanogenesis (21 min, with acetate). (C) Cells during active methanogenesis (21 min, with acetate) minus cells after cessation of linear methanogenesis (30 min, with acetate).

the washed cell suspension was found to be 0.18 mM by plasma emission spectroscopy. The pool of EPR-detectable cobalt thus appears to be the major pool of cobalt, and therefore corrinoid, in the cell.

Several changes coincident with methanogenesis can be seen in the region above $g = 2.0$ in the spectra taken at 70 K (Fig. 5). These signals could be observed at temperatures from 45 K to 95 K. Notable are the disappearance and reappearance of a feature at $g = 2.28$, the decrease in the intensity of features at $g = 2.22$ and 2.18, and the appearance of an intense signal at $g = 2.055$. Difference spectra in which the the spectra of actively methanogenic cells were subtracted from those of cells before the onset of methanogenesis show a clear rhombic signal at $g = 2.28$, 2.22, 2.18 (Fig. 6), the converse subtraction shows a strong feature at $g = 2.04$. These features are similar to two signals identified as Ni(I) of methylreductase in *Methanobacterium thermoautotrophicum* by Albracht and co-workers [33].

Effect of inhibitors of methanogenesis from acetate on paramagnetic centers

Cyanide is a potent inhibitor of methanogenesis from acetate, much more so than for methanogenesis from methanol or H_2 and CO_2 [12]. The effect has been attributed to the inhibition of CO dehydrogenase. We found that cyanide did induce EPR-detectable changes in CO dehydrogenase which correlated with cessation of methanogenesis from acetate. Methane formation by a suspension exposed to cyanide and acetate coincident with incubation at 37 °C is presented in Fig. 3. In the presence of cyanide, methane was initially evolved more slowly than in its absence, and ceased completely by 12 min. Center 2 was still observable 1 min after addition of cyanide, but by 10 min was no longer EPR detectable (Fig. 7). The loss of the feature was not accompanied by the appearance of the feature at $g = 1.73$, but was accompanied by a decrease in the intensity of the $g = 2.005$ feature, and a distinct broadening of the trough at $g = 1.89$. This was due to the development of a complex set of signals which could only be resolved below 8 K. Spectra taken at 6 K show that KCN induced formation of rapidly relaxing features at apparent g values of 2.05, 2.03, 1.96, 1.94, 1.91 and 1.88. These signals, as well as the loss of EPR-detectable center 2, could be observed independent of the presence of acetate. Spectra taken at 6 K of cells not exposed to either acetate or cyanide did not possess either of the fast relaxing centers, but were essentially similar to spectra taken at 12 K. We did not observe any cyanide induced changes in centers detectable by EPR at 70 K, including Co(II) corrinoid and the rhombic signal attributed to methylreductase.

We also investigated the effect of iodopropane inhibition of methane formation from acetate on EPR-detectable species. Fig. 8 illustrates a methane production curve for cells in the presence and absence of iodopropane. The inhibitor and acetate were added at the start

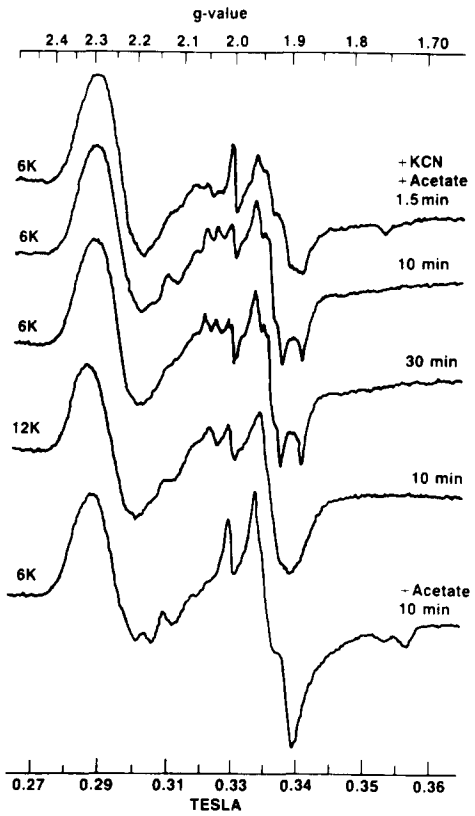

Fig. 7. EPR spectra recorded at 6 K and 12 K of *M. barkeri* exposed to cyanide. Methane formation from acetate by the cell suspension exposed to 50 μM cyanide is shown in Fig. 4, and samples for EPR were removed at the times indicated. The bottom spectrum is a sample from the uninhibited cell suspension. The temperature at which each spectrum was recorded is indicated to the left.

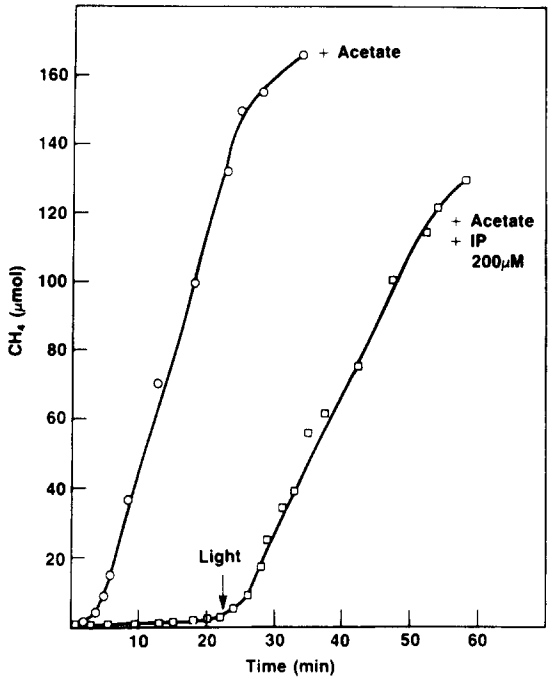

Fig. 8. Methane formation from cell suspensions in the presence and absence of iodopropane. Additions were made to 5 ml of cell suspension in aluminum foil wrapped vials at the start of incubation at 37 C. After 22 min, foil was removed and both vials were exposed to an 100 W incandescent bulb, 20 cm distant.

of incubation, and at 22 min inhibition was reversed by exposure to light. Iodopropane prevented the occurrence of methanogenesis related changes in EPR-detectable centers. However, no iodopropane-induced changes could be detected in any paramagnetic center, aside from intensification of the trough at $g = 2.00$. Spectra taken of inhibited cells at 12 K (fig. 9) or 70 K (data not shown) were essentially identical to cells not exposed to iodopropane. No decrease in the intensity of the Co(II) corrinoid signal could be detected despite the fact that sampling was performed in dim light and frozen samples were protected from exposure to light. Upon light reversal of inhibition, changes associated with the formation of methane could be observed, such as the decrease in the intensity of the $g = 1.76$ feature, the appearance of the $g = 1.73$ line, an increase in electron flow through iron-sulfur clusters, and the apparent interconversions of the two signals arising from methylreductase. The signal changes are therefore dependent on active methane formation and are not induced by the mere addition of acetate to intact cells.

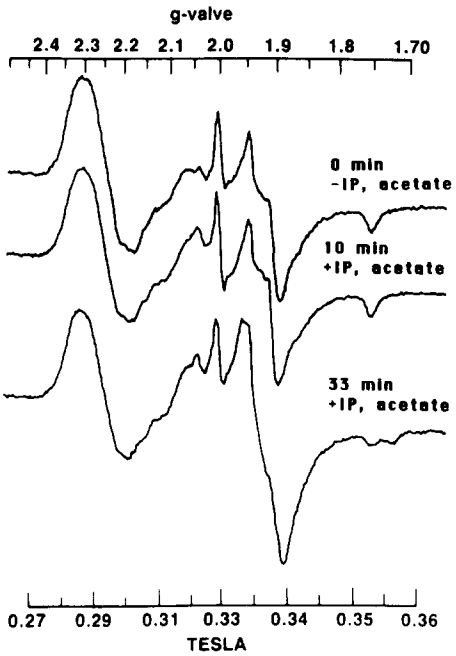

Fig. 9. EPR spectra of cells before and after light reversal of inhibition of methane formation by iodopropane. The spectrum labelled 0 min was taken of a cell suspension of ice before the addition of iodopropane and acetate. Other spectra are taken of the samples described in Fig. 8. All spectra were recorded at 12 K, 10 mW power, and a gain of $10 \cdot 10^3$.

Discussion

EPR detectable changes can be observed in carbon monoxide dehydrogenase when the enzyme is examined in intact cells during acetate catabolism, notably the decrease in the $g = 1.76$ feature and the appearance of a $g = 1.73$ line. Similar changes were noted in the isolated enzyme during exposure to carbon monoxide [26]. This strongly suggests that during methane formation from acetate an intermediate is generated which is recognized as carbon monoxide by carbon monoxide dehydrogenase. The approx. 50% decrease in the intensity of the $g = 1.76$ line indicates that, during steady-state methanogenesis, half the enzyme was in the form induced by carbon monoxide. The physical significance of the shift is unknown, and could be attributed to several events; such as, direct interaction of center 2 with water, or with either nucleus of a bound carbonyl moiety; or, a global conformational changes of the enzyme upon carbonyl binding. We cannot interpret our data further in this regard, since the intense signals due to iron-sulfur clusters interfere with observation of the other features of center 2 during acetate catabolism or in the presence of carbon monoxide. Understanding the nature of the shift should provide insight into the mechanism of carbon monoxide dehydrogenase. It is notable that the carbon monoxide dehydrogenases from *Clostridium thermoaceticum* [34] and *Rhodospirillum rubrum* [35] also possess centers with similar EPR signals, that is, g_{av} below 2.0 and a very high field g_x.

Our results show that carbon monoxide dehydrogenase is the site of cyanide inhibition of methane and carbon dioxide formation from acetate. Cells exposed to cyanide lost EPR-detectable center 2 coincident with cessation of methanogenesis. Center 2 is likely to remain reduced during turnover, since its $E_{m,9.2}$ is -35 mV. We have observed the reduced center at E_h as low

as −550 mV. Cyanide acts to convert the center into a non-detectable form, either by oxidation or destruction of the center. In any case, the center becomes unavailable for participation in the aceticlastic reaction.

The involvement of methylCoM in methanogenesis from acetate is well established. We have noted several changes in the lineshape of intact cell signals recorded at 70 K in the region between $g = 2.0$ and 2.3 before and after onset of methanogenesis. Difference spectra of resting and actively methanogenic cells indicate the signals are similar to the rhombic and axial signals identified as Ni(I) F_{430} in methylreductase from *Methanobacterium thermoautotrophicum* by Albracht et al. [33], which they termed MCR-red2, and MCR-red1, respectively. They proposed the difference between the two signals is axial ligation of HTP to F_{430} in the MCR-red2 form of the coenzyme, which is removed during production of methane and the heterodisulfide. Our data indicate that that MCR-red2 is seen only in resting cells, whereas MCR-red1 is predominant during methanogenesis, consistent with this suggestion. Further work is warranted to confirm the identity of these signals in *M. barkeri*.

During steady-state methanogenesis we observed no decrease in EPR-detectable corrinoid. In *Methanosarcina* strain Fusaro, 90% of the corrinoid is soluble, the remainder is membrane-bound [36]. At least 60% of the corrinoid in these cell suspensions was EPR-detectable, which suggests most of the signal arises from soluble corrinoid. Methylation of the isolated corrinoid from *M. barkeri* DSM 800 [30] or the corrinoid/iron-sulfur protein from *C. thermoaceticum* [37] results in EPR-silent Co(III). Thus, it appears that under conditions in which half of the carbon monoxide dehydrogenase was carbonylated, and much of methylreductase was in apparently active state, there was little steady-state methylation of this corrinoid pool. It appears certain that a corrinoid protein is involved in methanogenesis from acetate [21,22]. Our data suggest it is either not the major form of corrinoid in the cell, or is rapidly demethylated during acetate catabolism.

The Co(II) corrinoid signal was also unaffected by iodopropane at concentrations sufficient to inhibit methane formation. Significant alkylation of the corrinoid pool to EPR-silent Co(III) propylcorrinoid is therefore not a prerequisite of inhibition. The Co(II) corrinoid we observe is not the target of this specific, light reversible inhibition. It has been suggested that several corrinoids are present in *Methanosarcina*, only one of which is sensitive to inhibition by iodopropane [38]. If the site of inhibition is a corrinoid, it is apparently a minor species. It is notable that while two corrinoid proteins have been isolated from *Clostridium thermoaceticum* [37,39,40], only one serves as direct methyl donor to carbon monoxide dehydrogenase-dependent acetyl-CoA synthesis [37].

Acknowledgements

The authors wish to thank Dr. S.P.J. Albracht for his helpful discussions, in which he first noted the similarity between the signals we observed in *Methanosarcina* and his then unpublished spectra of methylreductase from *Methanobacterium*. We also thank him for the difference spectra he produced from our original data.

References

1 Jones, W.J., Nagle, D.P. and Whitman, W.B. (1987) Microb. Rev. 57, 135–177.
2 Stadtman, T.C. and Barker, H.A. (1949) J. Biochem. 21, 256–264.
3 Krzycki, J.A., Lehman, L. and Zeikus, J.G. (1985) J. Bacteriol. 160, 1000–1006.
4 Grahame, D.A. and Stadtman, T.C. (1987) Biochem. Biophys. Res. Commun. 147, 254–258.
5 Fischer, R. and Thauer, R.K. (1988) FEBS Lett. 228, 249–253.
6 Lovley, D.R., White, R.H. and Ferry, J.G. (1984) J. Bacteriol. 160, 521–525.
7 Krzycki, J.A. and Zeikus, J.G. (1985) FEMS Microbiol. Lett. 25, 27–32.
8 Zeikus, J.G., Kerby, R. and Krzycki, J.A. (1985) Science 227, 1167–2273.
9 Bott, M., Eikmanns, B. and Thauer, R.K. (1986) Eur. J. Biochem. 159, 393–398.
10 Peinemann, S., Müller, V., Blaut, M. and Gottschalk, G. (1988) J. Bacteriol. 170, 1369–1372.
11 Krzycki, J.A., Wolkin, R.H. and Zeikus, J.G. (1982) J. Bacteriol. 149, 247–254.
12 Smith, M.R., Lequerica, J.L. and Hart, M.R. (1985) J. Bacteriol. 162, 67–71.
13 Krzycki, J.A. and Zeikus, J.G. (1984) J. Bacteriol. 158, 287–292.
14 Ragsdale, S.W., Clark, J.E., Ljundahl, L.G., Lundie, L.L. and Drake, H.L. (1983) J. Biol. Chem. 258, 2364–2369.
15 DeMoll, E., Grahame, D.A., Harnly, J.M., Tsai, L. and Stadtman, T.C. (1987) J. Bacteriol. 169, 3916–3920.
16 Grahame, D.A. and Stadtman, T.C. (1987) J. Biol. Chem. 262, 3706–3712.
17 Terelesky, K.C., Nelson, M.J.K. and Ferry, J.G. (1986) J. Bacteriol. 168, 1053–1058.
18 Ragsdale, S.W. and Wood, H.G. (1985) J. Biol. Chem. 260, 3970–3977.
19 Krzycki, J.A. and Zeikus, J.G. (1980) Curr. Microbiol 3, 243–245.
20 Kenealy, W. and Zeikus, J.G. (1981) J. Bacteriol. 146, 133–140.
21 Eikmanns, B. and Thauer, R.K. (1985) Arch. Microbiol. 142, 175–179.
22 Van der Weingaard, W.M.H., Van der Drift, C. and G.D. Vogels, (1988) FEMS Microbiol. Lett. 52, 165–172.
23 Rouvière, P.E. and Wolfe, R.S. (1988) J. Biol. Chem. 263, 7913–7916.
24 Ellerman, J., Hedderich, R., Böcher, R. and Thauer, R.K. (1988) Eur. J. Biochem. 172, 669–677.
25 Bobik, T.A., Olson, K.D., Noll, K.M. and Wolfe, R.H. (1987) Biochem. Biophys. Res. Commun. 149, 455–460.
26 Krzycki, J.A., Mortenson, L.E. and Prince, R.C. (1989) J. Biol. Chem. 269, 7217–7221.
27 Bradford, M.M. (1976) Anal. Biochem. 72, 248–254.
28 Lino, A.R., Xavier, A.V., Moura, I., LeGall, J. and Moura, J.G. (1984) Rec. Chim. Pays-Bas 106, 350–351.
29 Schultz, H. Albracht, S.P.J., Coremans, J.M.C.C. and Fuchs, G. (1988) Eur. J. Biochem. 171, 579–597.
30 Lino, A.R., Xavier, A.V., Moura, I., LeGall, J. and Ljungdahl, L.G. (1985) Rev. Port. Quim. 27, 175–177.

31 Fauque, G., Teixeira, M., Moura, I., Lespinat, P.A., Xavier, A.V., DerVartanian, D.V., Peck, H.D., LeGall, J.L. and Moura, J.G. (1984) Eur. J. Biochem. 142, 21–28.
32 Kemner, J., Krzycki, J.A., Prince, R.C. and Zeikus, J.G. (1987) FEMS Microbiol. Lett. 48, 267–272.
33 Albracht, S.P.J., Ankel-Fuchs, D., Bocher, R., Ellermann, J., Moll. J., van der Zwaan, J.W. and Thauer, R.K. (1988) Biochim. Biophys. Acta 955, 86–102.
34 Ragsdale, S.W., Ljundahl, L.G., DerVartanian, D.V. (1982) Biochem. Biophys.Res. Commun. 108, 658–663.
35 Bonam, D. and Ludden, P.W. (1987) J. Biol. Chem. 262, 2980–2987.
36 Dangel, W. Schultz, H., Diekert, G., König, H. and Fuchs, G (1987) Arch. Microbiol. 148, 52–56.
37 Ragsdale, S.W., Lindahl, P.A. and Munck, E. (1987) J. Biol. Chem 269, 14289–14297.
38 Laufer, K., Eikmanns, B., Frimmer, U. and Thauer, R.K. (1987) Z Naturforsch. 42c, 360–372.
39 Ljungdahl, L.G., LeGall, J. and Lee, J.-P. (1973) Biochemistry 12 1802–1808.
40 Hu, S.-I., Pezacka, E. and Wood, H.G. (1984) J. Biol. Chem. 259 8892–8897.